REPORT 987

EQUILIBRIUM OPERATING PERFORMANCE OF AXIAL-FLOW TURBOJET ENGINES BY MEANS OF IDEALIZED ANALYSIS

By John C. Sanders and Edward C. Chapin

SUMMARY

A method of predicting equilibrium operating performance of turbojet engines has been developed, with the assumption of simple model processes for the components. Results of the analysis are plotted in terms of dimensionless parameters comprising critical engine dimensions and over-all operating variables.

This investigation was made for an engine in which the ratio of axial inlet-air velocity to compressor-tip velocity is constant, which approximates turbojet engines with axial-flow compressors.

Experimental correlation of the theory with data from several existing axial-flow-type engines was good and showed close correlation between calculated and measured performance.

INTRODUCTION

The equilibrium operating performance of a turbojet engine can be predicted from a knowledge of the component characteristics and the engine-design variables. A method of obtaining equilibrium performance is presented in reference 1. This method consists in considering the engine by its components (compressor, burner, turbine, and exhaust nozzle) and computing over-all performance from the given characteristics of each component. Because component characteristics are so complex and there are so many variables, computations based on available analyses are lengthy and are also limited to a single engine and operating point for any one series of calculations. A definite need exists for a more general form of analysis that will permit an approximate prediction of the performance of any engine configuration at any flight speed or altitude based on several critical dimensions and operating variables.

The first step in such an analysis is that of describing complicated component processes in some simplified manner. A method often successfully used is that of approximating actual processes by means of simple model processes with the final accuracy dependent on the degree of model refinement. Some work has already been done in approximating turbojet-component performance by means of model processes. Progress in the description of turbine performance by means of model processes is reported in reference 2.

An analysis in which the dimensions of the components are related to the performance of a turbojet engine was made at the NACA Lewis laboratory during 1948 and is presented herein. The results are presented in such a fashion that they are applicable to any turbojet engine. This general presentation requires a knowledge of the efficiencies of the individual components, compressor and turbine, under various operating conditions. The performance of turbojet engines for constant efficiencies of compressor and turbine may be read directly from the general presentation. Superimposition of compressor and turbine characteristics upon the general presentation permits accurate calculation of the performance. Results of the analysis are compared with experimental data.

This analysis is of interest for three reasons:

(1) It is a step toward a rational calculation of turbojet-engine performance, the full realization of which will permit calculation of performance from the drawings of the engine.

(2) The generalized presentation shows how variations in important design and operating parameters will influence performance.

(3) The analysis affords a method of accurately matching compressors and turbines for which the performance characteristics are known in detail.

SYMBOLS

The following symbols are used in this report:

A	cross-sectional area, square feet
A_t	turbine minimum-passage area, square feet
a	velocity of sound based on total temperature, feet per second
C	constant
D	compressor-rotor-blade-tip diameter, feet
F	net thrust, pounds
f	fuel-air ratio plus 1
hp	horsepower
K_c	ratio of inlet-air velocity to compressor-blade-tip velocity
M_c	compressor-blade-tip Mach number based on inlet temperature
$M_{c,0}$	compressor-blade-tip Mach number based on ambient temperature
M_0	flight Mach number based on ambient temperature
N	engine speed, rpm
P	total pressure, pounds per square foot absolute
p	static pressure, pounds per square foot absolute
Q	air flow, cubic feet per second
R	gas constant, foot-pounds per slug °R
r	total-pressure ratio
T	total temperature, °R

V velocity, feet per second

V_c compressor-blade-tip velocity, feet per second

W mass flow, slugs per second

γ ratio of specific heat at constant pressure to specific heat at constant volume

δ ratio of compressor-inlet absolute total pressure to NACA standard sea-level absolute pressure

η efficiency

θ ratio of compressor-inlet absolute total temperature to NACA standard sea-level absolute temperature

ρ mass density, slugs per cubic foot

ψ pressure coefficient

Subscripts:

b burner

c compressor

j jet

n nozzle

r ram

t turbine

0 ambient

1 compressor inlet

2 compressor outlet

3 turbine inlet

4 turbine outlet

5 nozzle outlet

ANALYSIS

DESCRIPTION OF COMPONENT MODELS

In order to establish theoretical equilibrium operating conditions, the performance of each engine component must be described. The descriptive equations for each component and the development of the analysis are given in the appendix. The principal equations of the analysis are described in the following paragraphs.

EQUILIBRIUM PERFORMANCE

The assumptions are now stated and all descriptive equations are combined to define equilibrium operating performance of the complete engine.

Assumptions.—Equation (3) is used as an approximation for W_t in order to avoid complications in the equilibrium analysis. For low-reaction turbines and turbines operating at or near choking conditions, the approximation is of sufficient accuracy. A further assumption made using equation (3) is that the turbine pressure ratio used in calculating equilibrium performance is considered to be the total-pressure ratio from the inlet to the outlet of the turbine. The turbine pressure ratio in equation (3) should be the total-to-static pressure ratio across the turbine; however, the error in this assumption is small. Figure 1 shows the magnitude

Compressor.—The development of the analysis requires that a simple expression for compressor mass flow be known. The ratio of inlet-air velocity to compressor-blade-tip velocity K_c for axial-flow compressors has been found to be approximately constant, particularly at or near design speed. Hence, with the use of this relation, the following expression for compressor air flow W_c can be developed:

$$\frac{W_c\sqrt{T_0}}{P_0}=K_cM_cA_c(r_t)^{\frac{\gamma_c+1}{2\gamma_c}}\sqrt{\frac{\gamma_c}{R}} \qquad (1)$$

The power to drive the compressor may be expressed as

$$\mathrm{hp}_c=\frac{W_c}{550\,\eta_c}\left(\frac{\gamma_c}{\gamma_c-1}\right)RT_0(r_r)^{\frac{\gamma_c-1}{\gamma_c}}\left[(r_c)^{\frac{\gamma_c-1}{\gamma_c}}-1\right] \qquad (2)$$

Turbine.—In order to obtain a simplified expression for the gas flow through the turbine W_t, the turbine and the turbine nozzle were considered similar to a simple channel of varying cross section. The expression for W_t is then written as

$$\frac{W_t\sqrt{T_0}}{P_0}=\sqrt{\frac{2\gamma_t}{\gamma_t-1}}\frac{A_t}{\sqrt{R}}\left(\frac{T_0}{T_3}\right)^{\frac{1}{2}}\frac{r_c r_r}{r_b}\left[\left(\frac{C}{r_t}\right)^{\frac{2}{\gamma_t}}-\left(\frac{C}{r_t}\right)^{\frac{\gamma_t+1}{\gamma_t}}\right]^{\frac{1}{2}} \qquad (3)$$

The turbine power may be expressed as

$$\mathrm{hp}_t=\frac{W_t}{550}\,\eta_t\left(\frac{\gamma_t}{\gamma_t-1}\right)RT_3\left[1-\left(\frac{1}{r_t}\right)^{\frac{\gamma_t-1}{\gamma_t}}\right] \qquad (4)$$

(Herein, A_t is the turbine minimum-passage area.)

Exhaust nozzle.—The exhaust nozzle is described in the same manner as the turbine and the equation for the flow through the exhaust nozzle becomes

$$\frac{W_n\sqrt{T_0}}{P_0}=\sqrt{\frac{2\gamma_t}{(\gamma_t-1)R}}\frac{A_n}{(r_t)^{\frac{\gamma_t+1}{2\gamma_t}}}\frac{r_r r_c}{r_b}\left(\frac{T_0}{T_3}\right)^{\frac{1}{2}}\left[\left(\frac{r_t r_b}{r_r r_c}\right)^{\frac{2}{\gamma_t}}-\left(\frac{r_t r_b}{r_c r_r}\right)^{\frac{\gamma_t+1}{\gamma_t}}\right]^{\frac{1}{2}} \qquad (5)$$

of error in using r_t as the total-to-total pressure ratio in the expression

$$\left[\left(\frac{1}{r_t}\right)^{\frac{2}{\gamma_t}}-\left(\frac{1}{r_t}\right)^{\frac{\gamma_t+1}{\gamma_t}}\right]^{\frac{1}{2}}$$

rather than the total-to-static pressure. The error reaches a maximum of about 5 percent at low values of r_t. If a more accurate solution is required, a factor C can be included in equation (3), as shown, to correct the error.

The burner pressure ratio r_b appearing in equations (3) and (5) represents a measure of the pressure drop in the burner. In order to make the equations as simple as possible, this pressure ratio was included rather than a more complicated equation for the loss.
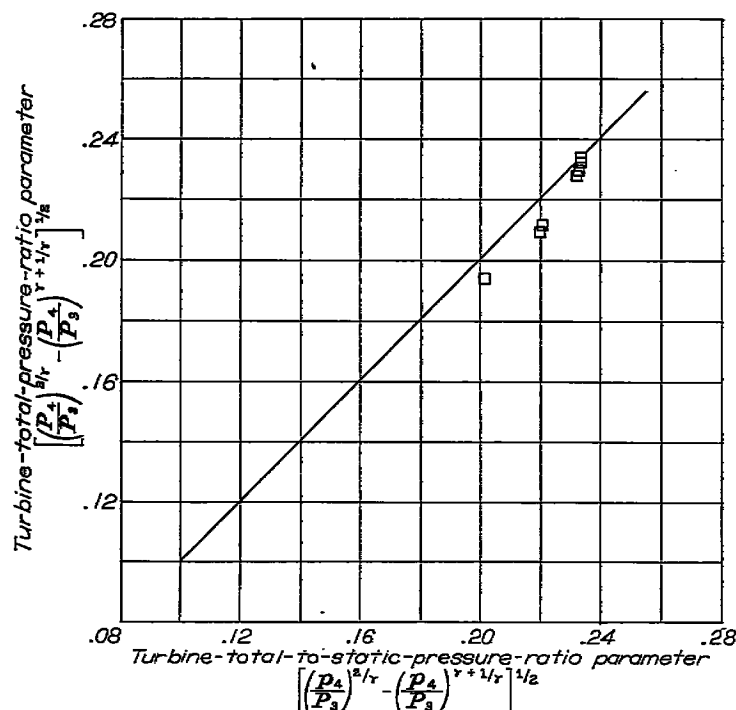
FIGURE 1.—Relation between turbine-total-pressure-ratio parameter and total-to-static-pressure-ratio parameter. Turbojet engine A.

The areas A_t and A_n in equations (3) and (5), respectively, are effective flow areas rather than actual passage areas. These areas were calculated using equations (3) and (5) and

observed engine data. Experimental variation from average values of A_n/A_t for two engines is plotted against engine speed N in figure 2.

In the development of equation (5), the turbine-outlet temperature T_4 was determined assuming the turbine temperature drop to be isentropic. Thus, the turbine-outlet temperature used in the theoretical calculations is somewhat lower than the actual temperature. The error involved in making this assumption, however, is small and can be neglected. (See reference 3.)

Equilibrium.—In order to establish equilibrium operation of a turbojet engine, two general conditions must be satisfied. The compressor air flow plus fuel flow must equal the gas flow through the turbine and the exhaust nozzle, and the power delivered by the turbine must equal the power necessary to drive the compressor. In this analysis, no air is assumed to leave the system and no mechanical losses are assumed to be incurred. From these relations and the five equations developed from the component-model analysis, equations may be developed that define equilibrium performance of the complete turbojet engine.

Equating the two expressions for mass flow (equations (1) and (3)) and the power expressions (equations (2) and (4)) provides two separate expressions for the compressor pressure ratio r_c. The equation for equilibrium operation can be determined by setting the two equations for r_c equal to each other:

$$\left\{ 1 + f \frac{\gamma_t(\gamma_c-1)}{\gamma_c(\gamma_t-1)}\left(\frac{T_3}{T_0}\right)\frac{\eta_c\eta_t}{(r_r)^{\frac{\gamma_c-1}{\gamma_c}}}\left[1-\left(\frac{1}{r_t}\right)^{\frac{\gamma_t-1}{\gamma_t}}\right]\right\}^{\frac{\gamma_c}{\gamma_c-1}}\left[\left(\frac{C}{r_t}\right)^{\frac{2}{\gamma_t}}-\left(\frac{C}{r_t}\right)^{\frac{\gamma_t+1}{\gamma_t}}\right]^{\frac{1}{2}} = \frac{A_c}{A_t}f\frac{K_cM_cr_b}{(r_r)^{\frac{\gamma_c-1}{2\gamma_c}}}\left(\frac{T_3}{T_0}\right)^{\frac{1}{2}}\sqrt{\frac{\gamma_c(\gamma_t-1)}{2\gamma_t}} \quad (6)$$

With the assumption of constant values for γ_c, γ_t, and r_b, and with r_r held constant for any one series of calculations, equation (6) expresses the speed parameter $\frac{A_c}{A_t}fK_cM_c\left(\frac{T_3}{T_0}\right)^{\frac{1}{2}}$ as a function of the temperature parameter $f(T_3/T_0)\eta_t\eta_c$ and r_t.

The turbine pressure ratio r_t can be combined with r_c and the quantity r_c/r_t plotted against functions of engine speed and temperature to indicate the pumping capacity of any compressor-turbine configuration.

In this analysis, however, it is of more interest to develop a correlation of nozzle-to-turbine minimum-passage-area ratio A_n/A_t as a function of engine speed and temperature.

Hence, by combination of equations (3) and (5), the following expression for A_n/A_t can be developed in terms of r_t:

$$\frac{A_n}{A_t} = \frac{(r_t)^{\frac{\gamma_t+1}{2\gamma_t}}\left[\left(\frac{C}{r_t}\right)^{\frac{2}{\gamma_t}}-\left(\frac{C}{r_t}\right)^{\frac{\gamma_t+1}{\gamma_t}}\right]^{\frac{1}{2}}}{\left[\left(\frac{r_tr_b}{r_rr_c}\right)^{\frac{2}{\gamma_t}}-\left(\frac{r_tr_b}{r_rr_c}\right)^{\frac{\gamma_t+1}{\gamma_t}}\right]^{\frac{1}{2}}} \quad (7)$$

After the equilibrium operating conditions have been established, the analysis can be expanded to provide specific performance figures. As an example, an expression for engine net thrust per unit turbine area F/P_0A_t is developed in the appendix. The final expression for this quantity is given in the following equation:

$$\frac{F}{P_0A_t} = \frac{A_c}{A_t}K_cM_c(r_r)^{\frac{\gamma_c+1}{2\gamma_c}}\gamma_c\left\{f\sqrt{\frac{2\gamma_t}{\gamma_c(\gamma_t-1)}\left(\frac{T_3}{T_0}\right)\left(\frac{1}{r_t}\right)^{\frac{\gamma_t-1}{\gamma_t}}\left[1-\left(\frac{r_tr_b}{r_cr_r}\right)^{\frac{\gamma_t-1}{\gamma_t}}\right]}-M_0\right\} \quad (8)$$

GENERALIZED EQUILIBRIUM CHARTS

Equilibrium operating lines.—The general solution of the equilibrium equations is shown in figure 3 in which the speed parameter $\frac{A_c}{A_t}K_cM_c\left(\frac{f}{\eta_c\eta_t}\right)^{\frac{1}{2}}$ is plotted against the tempera-

ture parameter $f\frac{T_3}{T_0}\eta_c\eta_t$ for three values of A_n/A_t and two values of r_r.

Experimental data indicated that the pressure loss in the burner had to be accounted for in establishing correct equilibrium performance. The average value of pressure ratio
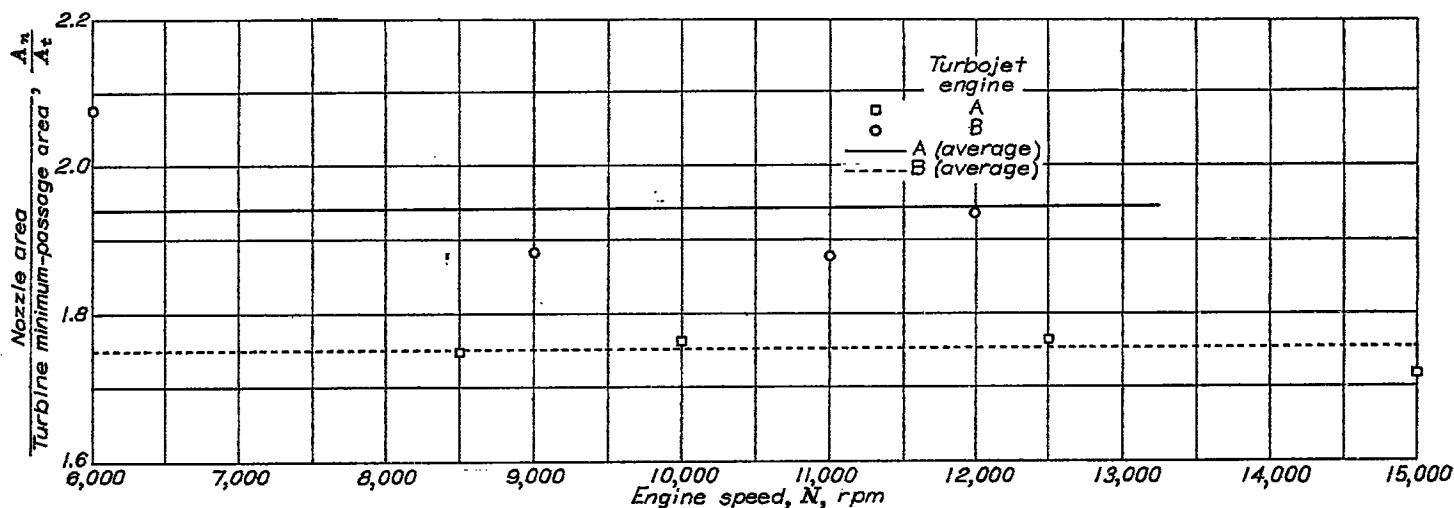
FIGURE 2.—Experimental variation of ratio of nozzle area to turbine minimum-passage area with engine speed for two turbojet engines.
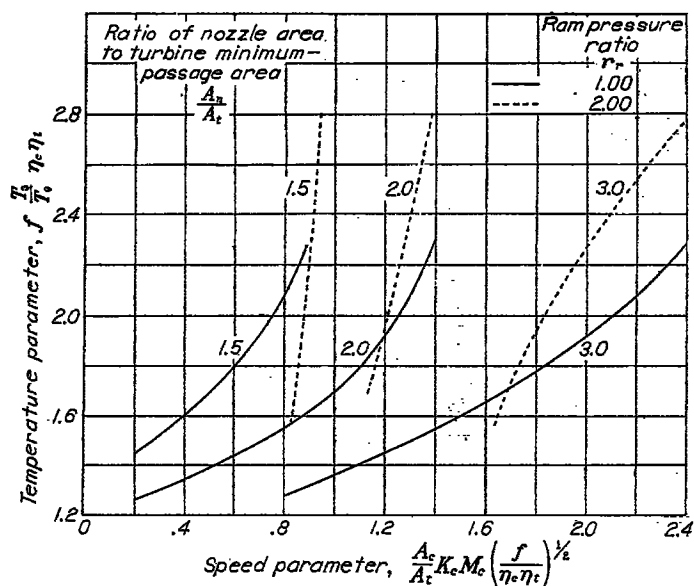

FIGURE 3.—General solution of equilibrium equations for several ratios of nozzle area to turbine minimum-passage area and two ram pressure ratios with the assumption of no burner pressure loss.
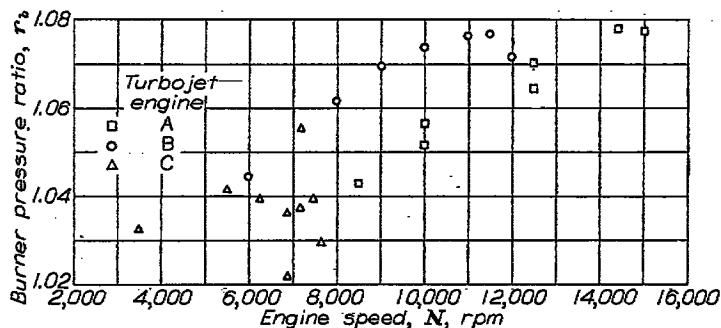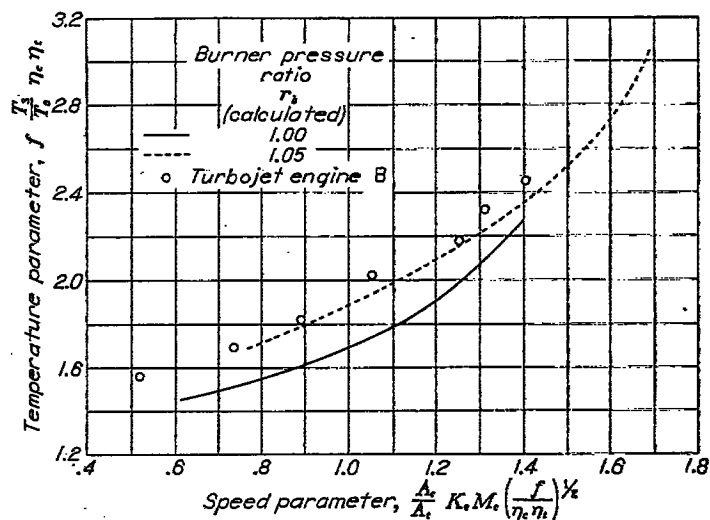

FIGURE 5.—Comparison of experimental data and calculated equilibrium operating lines for two assumed burner pressure ratios. Ratio of nozzle area to turbine minimum-passage area, 1.96; ram pressure ratio, 1.04.

FIGURE 4.—Experimental variation of burner pressure ratio with engine speed for three turbojet engines.

across the burner was used (fig. 4) rather than a more complicated factor for this loss.

A comparison of experimental data from an axial-flow-type engine with the theoretical curves calculated for no pressure loss in the burner (r_b of 1.00) and for an assumed constant r_b of 1.05 is shown in figure 5. Similar correlation was made with data from other engines, indicating that in-

clusion of this constant factor of 1.05 made the theoretical curves sufficiently accurate for most purposes.

The effect of burner pressure loss, indicated by the burner pressure ratio r_b, on the theoretical equilibrium operating lines for values of ram pressure ratio of 1.00 and 2.00 is shown in figure 6. This loss in the burner has the greatest effect at low values of the speed parameter $\frac{A_c}{A_t} K_c M_c \left(\frac{f}{\eta_c \eta_t}\right)^{\frac{1}{2}}$ and at low ram pressure ratios. At high ram pressure ratios, the burner pressure loss has a very small effect on equilibrium operation. Hence, for current engine designs and probable future designs, the assumption of a constant r_b is of reasonable accuracy. For engines operating at low speeds and temperature ratios, the assumption becomes less accurate.

Equilibrium for r_r values of 1.00 and 2.00 and for several different values of A_n/A_t for a burner pressure ratio of 1.05 is shown in figure 7. All subsequent experimental verifications are based on this chart. If all the parameters were known, this type of chart would permit a general exploration of the effects of component dimensions and operating variables on the equilibrium operating performance of any turbojet engine.
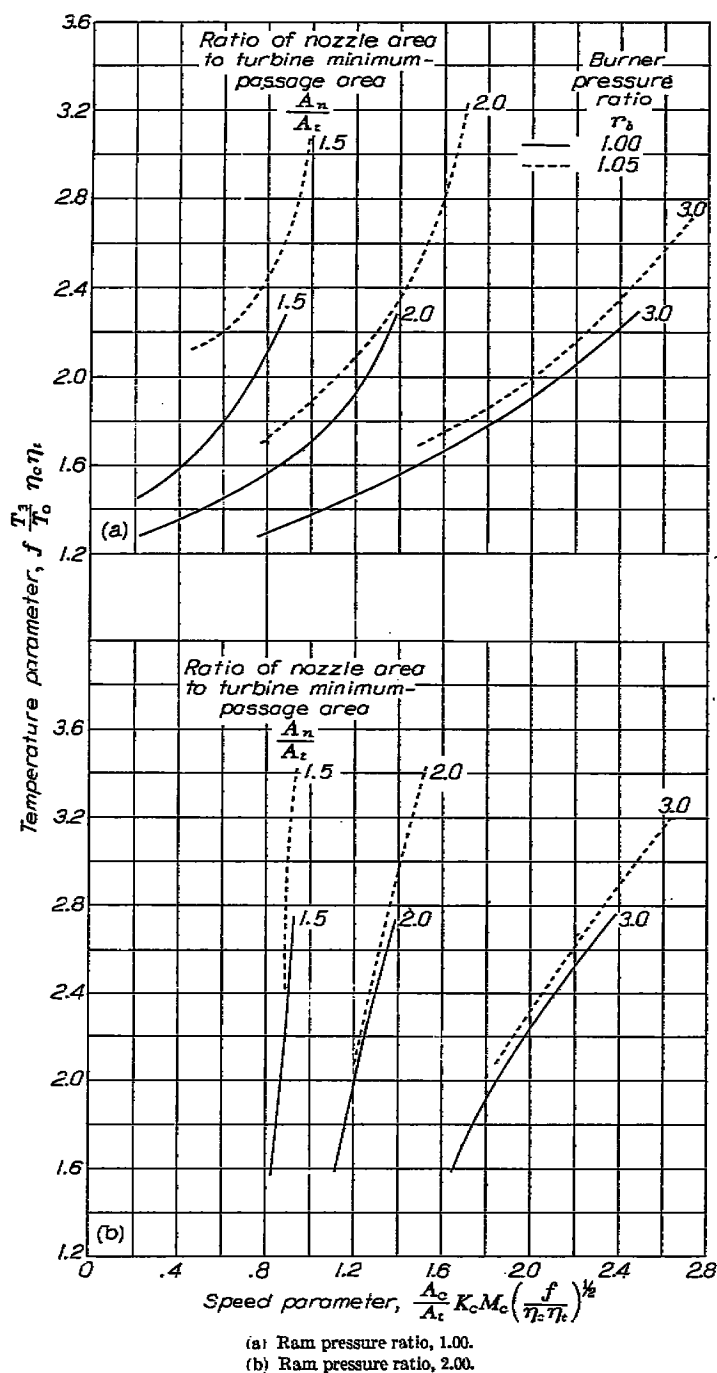
Figure 6.—Effect of burner pressure ratio on general equilibrium operating line for several ratios of nozzle area to turbine minimum-passage area and two ram pressure ratios.
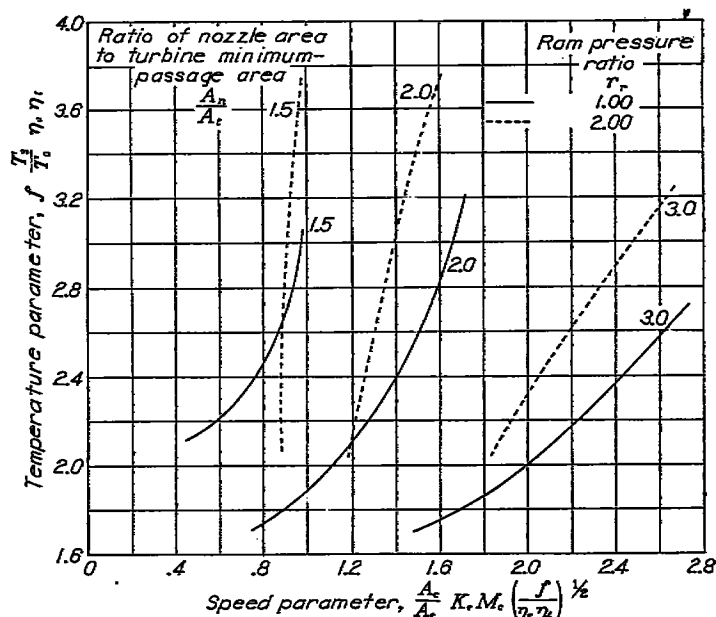

Figure 7.—Equilibrium operating lines for turbojet engine with several ratios of nozzle area to turbine minimum-passage area and two ram pressure ratios. Burner pressure ratio, 1.05.
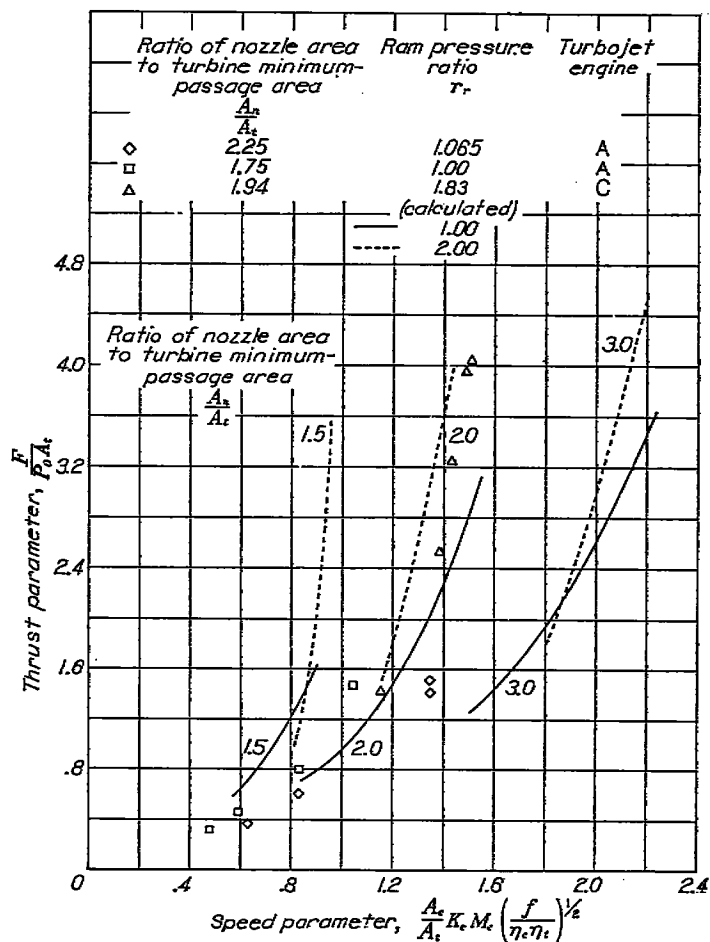

Figure 8.—Effect of speed parameter on turbojet-engine thrust for several ratios of nozzle area to turbine minimum-passage area and two ram pressure ratios. Burner pressure ratio, 1.05.

Net thrust.—After the equilibrium analysis is made, it is possible to use the resultant knowledge of component performance in calculating the over-all performance factors, such as net thrust. Figure 8 shows theoretical curves of

$F/P_o A_t$ plotted against the speed parameter $\frac{A_c}{A_t} K_c M_c \left(\frac{f}{\eta_c \eta_t}\right)^{\frac{1}{2}}$.

These curves include the constant burner-pressure-drop factor. In order to determine $F/P_o A_t$ from this analysis, the efficiency product $\eta_c \eta_t$ must be assumed constant when points are desired at flight speeds other than zero. The accuracy of this assumption is subsequently discussed.

EXPERIMENTAL VERIFICATION OF THEORETICAL CURVES

With the theoretical equilibrium performance now established, the theoretical equilibrium operating lines may be compared with experimental data.

Experimental data from several turbojet engines having different area ratios are shown in figure 9 compared with the theoretical equilibrium operating lines. The theoretical curves were made assuming constant ratios of specific heats
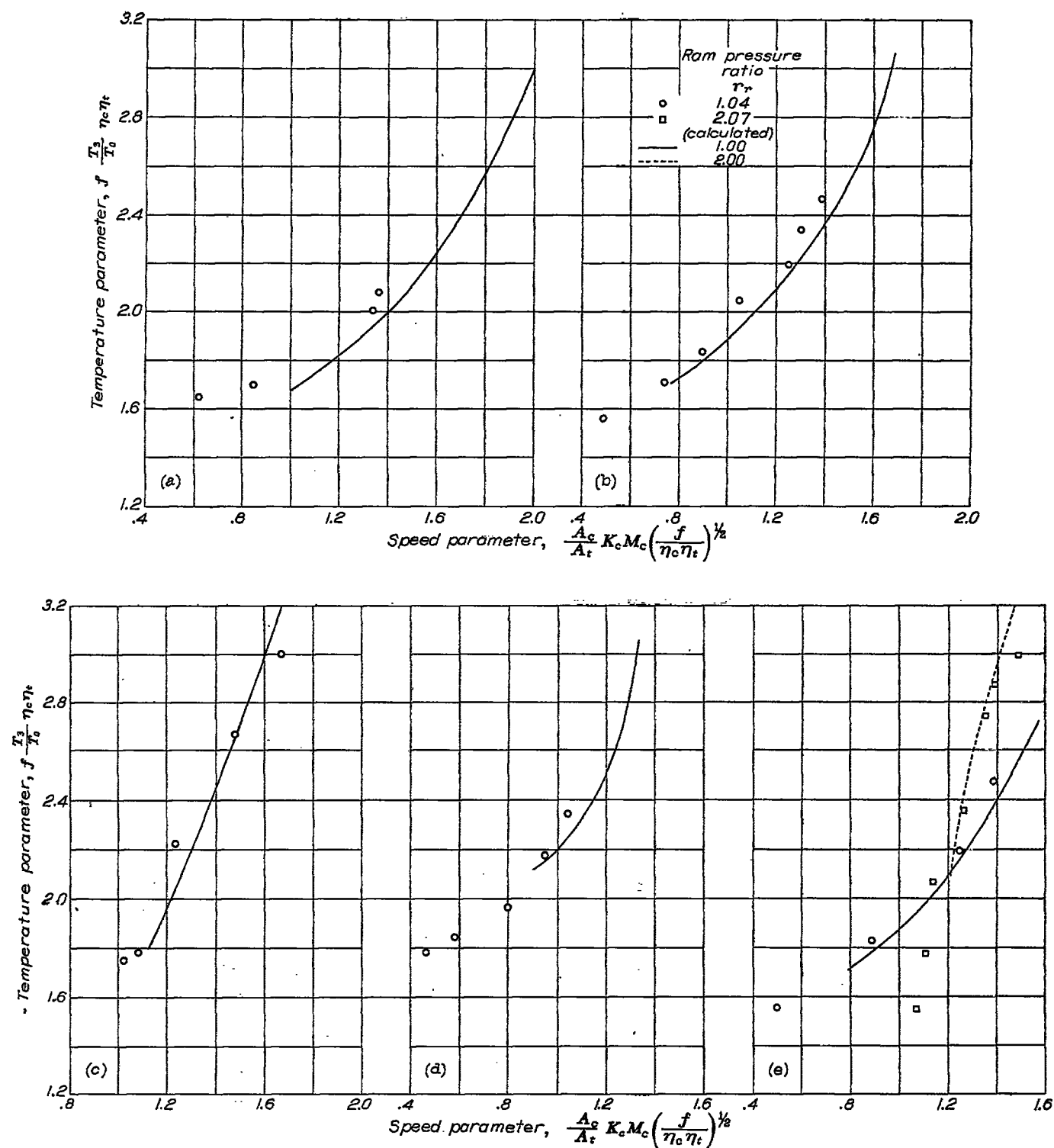
(a) Turbojet engine A; ratio of nozzle area to turbine minimum-passage area, 2.25; ram pressure ratio, 1.00.

(b) Turbojet engine B; ratio of nozzle area to turbine minimum-passage area, 1.96; ram pressure ratio, 1.04.

(c) Turbojet engine C; ratio of nozzle area to turbine minimum-passage area, 1.04; ram pressure ratio, 1.20.

(d) Turbojet engine A; ratio of nozzle area to turbine minimum-passage area, 1.75; ram pressure ratio, 1.00.

(e) Turbojet engine B; ratio of nozzle area to turbine minimum-passage area, 1.96; ram pressure ratios, 1.04 and 2.07.

FIGURE 9.—Comparison of calculated equilibrium operating lines and experimental data for several turbojet engines. Burner pressure ratio, 1.05.

of 1.40 and 1.32 in the compressor and turbine, respectively. A constant burner pressure ratio of 1.05 was used and the areas were assumed to be effective flow areas.

The experimental data points were calculated using average values of effective areas and observed values of K_c at each data point. Experimental correlation is good enough to make the assumptions used in the analysis appear to be within reasonable accuracy. Hence, the equilibrium operating lines can be considered as accurate as the parameters and applicable to any turbine-type engine.

Further use can be made of the equilibrium charts if K_c and $\eta_c\eta_t$ are constant for a particular engine or if a means is available for determining the values of these quantities at any desired operating point.

Assumption of constant K_c.—Many compressors have a constant ratio of axial inlet-air velocity to compressor-tip velocity K_c in at least some part of the operating range. Figure 10 is a replot of figure 9(e) except that in this figure
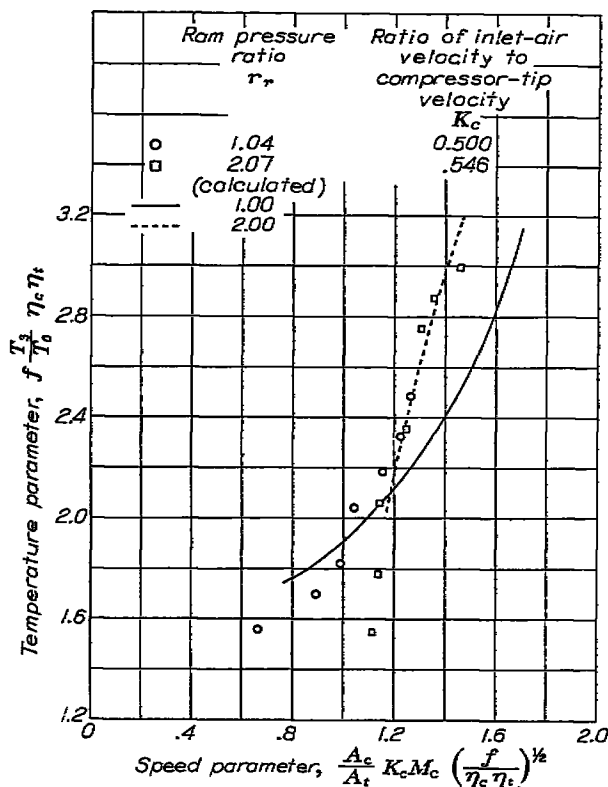

FIGURE 10.—Effect of assuming constant ratio of axial inlet-air velocity on correlation between calculated equilibrium operating line and experimental data. Turbojet engine B; ratio of nozzle area to turbine minimum-passage area, 1.96.

the K_c used in calculating the experimental speed parameter was an average value. Experimental correlation is still good when the engine is operating at high flight speed but is poorer as flight speed is reduced. This effect can be partly explained by figure 11, which shows how the equilibrium operating line shifts on the compressor-performance map when the ram pressure is changed. At high r_r values, the operating line moves lower on the constant engine-speed lines into the more vertical portion of the curves where the assumption of constant K_c becomes more accurate.

Assumption of constant $\eta_c\eta_t$.—When the equilibrium curves are used to determine dimensional effects upon temperature ratio and engine speed, a knowledge of the variation in the
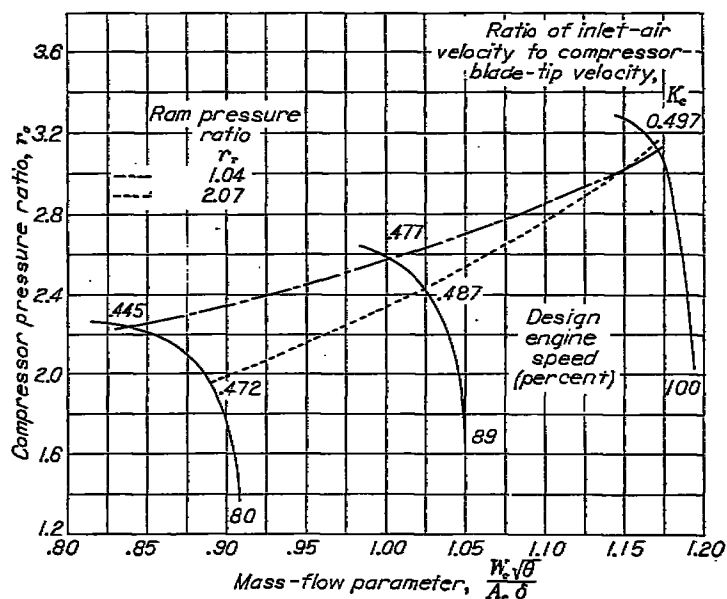

FIGURE 11.—Effect of ram pressure ratio on position of equilibrium operating line on compressor-performance map. Turbojet engine B; ratio of nozzle area to turbine minimum-passage area, 1.96.

efficiency product $\eta_c\eta_t$ is necessary. In many instances this product may be known at all points of operation. When an assumption of this product must be made, constant $\eta_c\eta_t$ may be of sufficient accuracy. Figure 12 shows the variation of $\eta_c\eta_t$ with N for an engine having two different exhaust-nozzle areas and indicates that assumption of constant $\eta_c\eta_t$ for these engines is within reasonable accuracy.
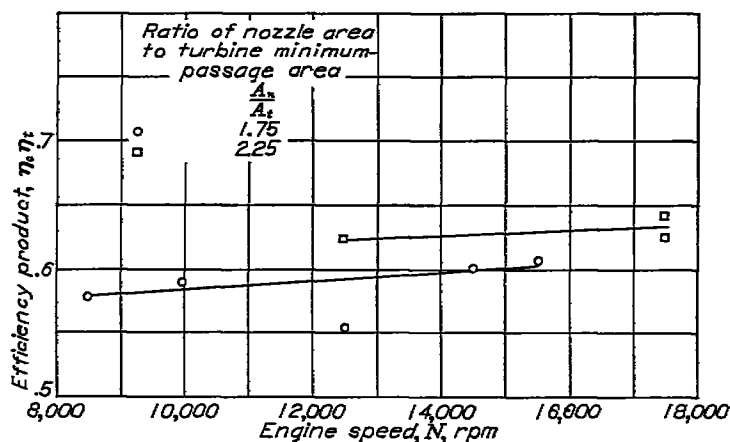

FIGURE 12.—Experimental variation of efficiency product with engine speed. Turbojet engine A; ram pressure ratio. 1.00.

If values of K_c and $\eta_c\eta_t$ are known at each operating point, the theoretical curves agree fairly well with the experimental data. An assumption of constant K_c for an axial-flow-type engine is reasonably accurate for engines operating at high flight speed, especially near the design engine speed.

DISCUSSION

With the general results of the analysis completed, many more results can be developed from the main calculations. Three of these developments are discussed.

Analysis for engine speed limited by stress.—In all the curves presented so far, the speed parameter $\dfrac{A_c}{A_t}K_cM_c\left(\dfrac{f}{\eta_c\eta_t}\right)^{\frac{1}{2}}$

has included the Mach number of the compressor-blade tip M_c based on the compressor-inlet total temperature. Hence, vertical lines drawn from the abscissa of the equilibrium charts are lines of constant compressor-tip Mach number provided that the other factors in the speed parameter remain constant. This form of presentation is most practical when the compressor-tip Mach number is considered to limit engine speed. If stresses limit the rotational speed, a speed parameter containing engine speed would be more desirable. Figures 13 and 14 show equilibrium lines and thrust lines, respectively, using a speed parameter with M_c replaced by a Mach number $M_{c,0}$ based on ambient temperature. Vertical lines using this new speed parameter represent lines of constant N if the other factors in the parameter remain constant.

Variation of exhaust-nozzle area.—If an engine has a variable-area exhaust nozzle, the equilibrium curves of figures 7 and 13 would be useful in determining the correct exhaust-nozzle area A_n for different altitudes and ram pressures. The correct nozzle area can be determined, depending on the particular region of operation on the charts, the ram pressure, the altitude, and the engine-speed limiting factors. For example, assume that it is required to determine the A_n necessary to maintain either constant N or constant M_c when r_r is increased from 1.00 to 2.00. When the engine is assumed to be operated initially with an r_r of 1.00, an A_n/A_t of 2.0, and a $f\frac{T_3}{T_0}\eta_c\eta_t$ of 2.1, the two speed parameters previously mentioned are equal and have a value of approximately 1.2. (See figs. 7 and 13.) If an r_r of 2.00 is applied to the engine, A_n does not have to be changed to operate at constant M_c (fig. 7). If N is to be maintained constant, however, it can be seen from figure 13 that A_n must be de-

FIGURE 14.—Variation of thrust parameter with speed parameter based on ambient temperature for several ratios of nozzle area to turbine minimum-passage area and two ram pressure ratios. Burner pressure ratio, 1.05.

creased to maintain the same parameters at an r_r of 2.00. The same type of analysis of proper nozzle area can be carried out on figure 14 to determine the thrust parameter. Because the equilibrium lines for the two ram pressure ratios cross, depending on the operating range, A_n might be increased or decreased for correct operation when r_r is changed. The correct exhaust-nozzle area can be determined for each altitude by a similar type of analysis using these charts.

Incorporation of observed component characteristics.— The chart of figure 7 describes the equilibrium operating performance of any turbojet engine. By further expansion of the analysis, however, this chart may be modified to allow superimposition of specific compressor and turbine maps on the generalized equilibrium performance chart. The addition of values of r_c on the chart permits more accurate and complete performance predictions for a specific compressor-turbine combination. Lines of constant compressor pressure ratio r_c and constant turbine ratio are shown in figure 15.

With the addition of lines of constant r_c and r_t on the equilibrium performance chart, it is now possible to superimpose on the chart compressor and turbine performance characteristics with the assumption of a specified temperature ratio at the design point. Because an original assumption of η_t must be made to initiate the calculations, several repeated calculations are necessary to match the compressor and the turbine accurately on the equilibrium performance chart. The compressor efficiency η_c, velocity ratio indicated by CK_c, and the surge line obtained from experimental data on a compressor are shown in figure 16. Similarly, figure 17
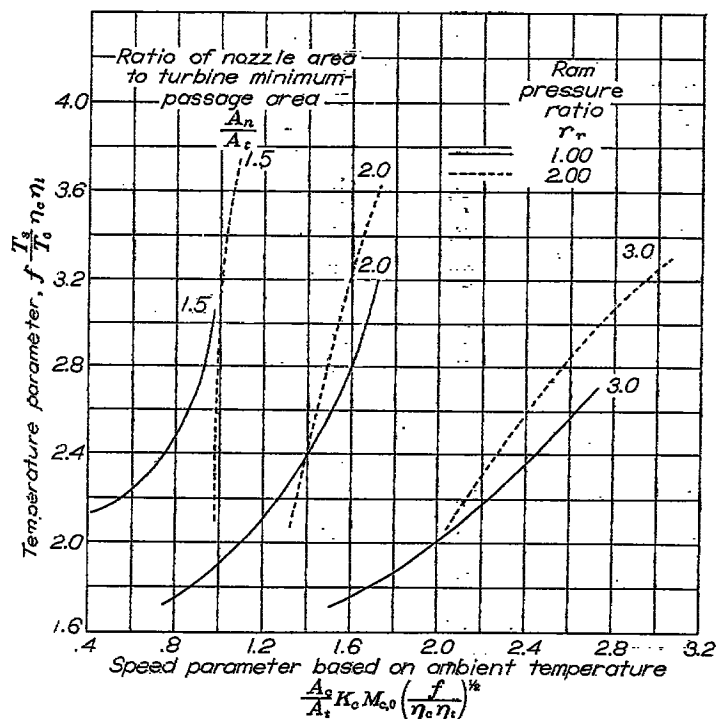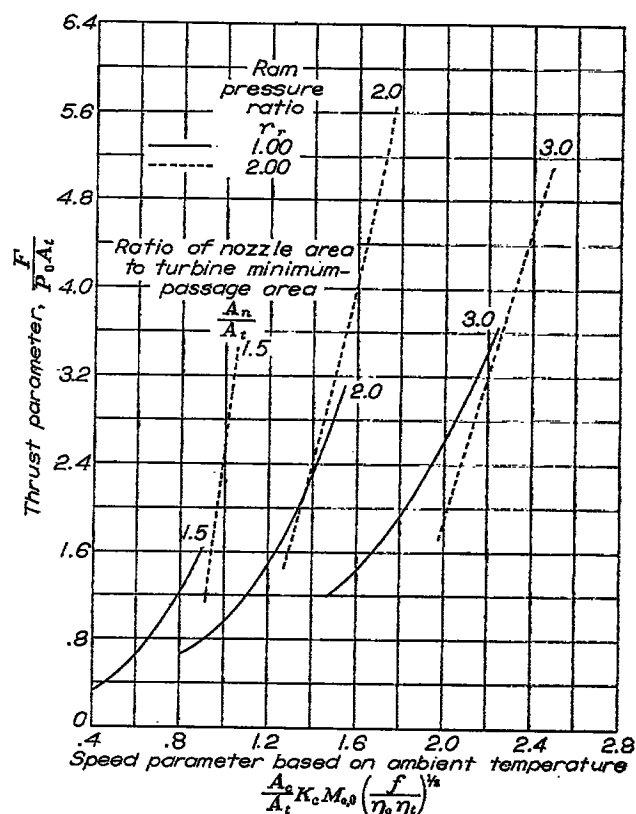

FIGURE 13.—Variation of equilibrium operating lines with speed parameter based on ambient temperature for several ratios of nozzle area to turbine minimum-passage area and two ram pressure ratios. Burner pressure ratio, 1.05.

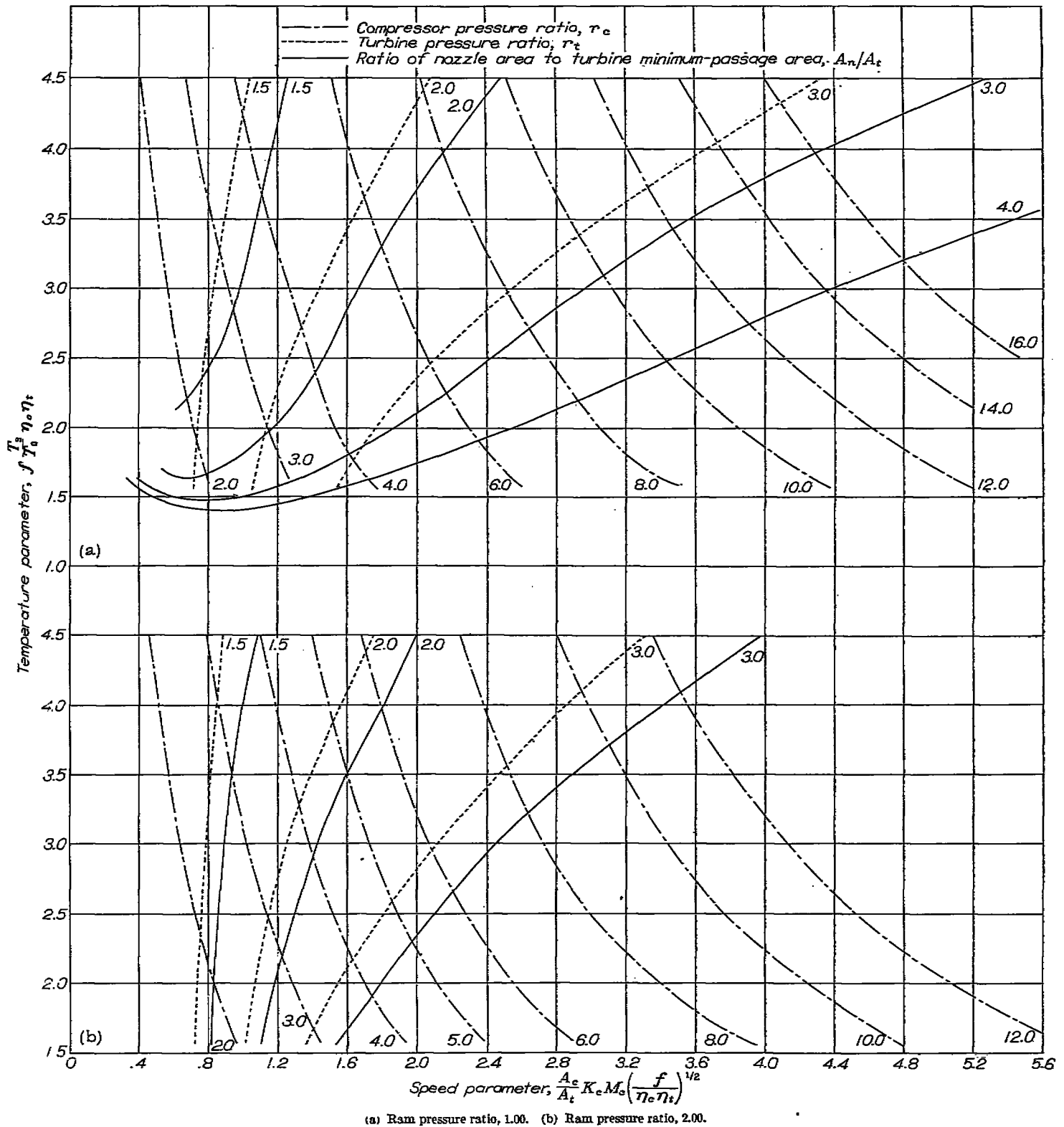(a) Ram pressure ratio, 1.00.   (b) Ram pressure ratio, 2.00.

FIGURE 15.—General equilibrium curves showing lines of constant compressor pressure ratio and turbine pressure ratio for several ratios of nozzle area to turbine minimum-passage area and two ram pressure ratios. Burner pressure ratio, 1.05.

shows the efficiency contours for a selected turbine. Figures 16 and 17 thus contain sufficiently complete information on component characteristics to permit accurate determination of equilibrium performance but still retain the more general equilibrium performance.

SUMMARIZING REMARKS

It has been shown that it is possible to determine equilibrium performance of a turbojet engine by means of simple model processes developed for each of the components.

The results are presented in a series of graphs with equilibrium engine performance plotted in terms of temperature ratio, engine speed, flight Mach number, and component dimensions, such as ratio of compressor-inlet area to turbine minimum-passage area and ratio of turbine minimum-passage area to exhaust-nozzle area.

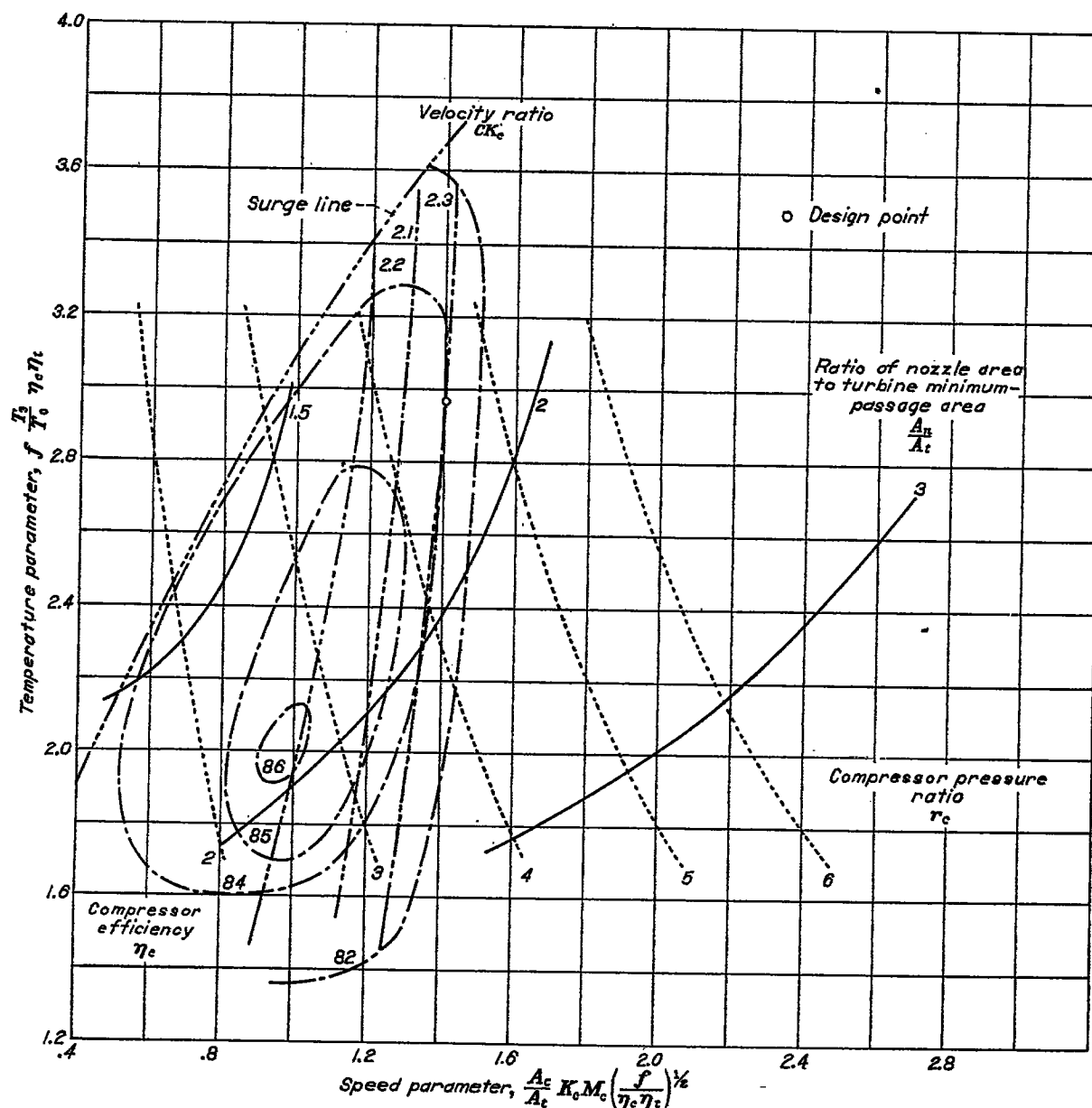The analysis is expanded further to permit calculation of

FIGURE 16.—Compressor-component characteristics from compressor data with equilibrium operating lines. Ram pressure ratio, 1.00; burner pressure ratio, 1.05. C, proportionality constant.
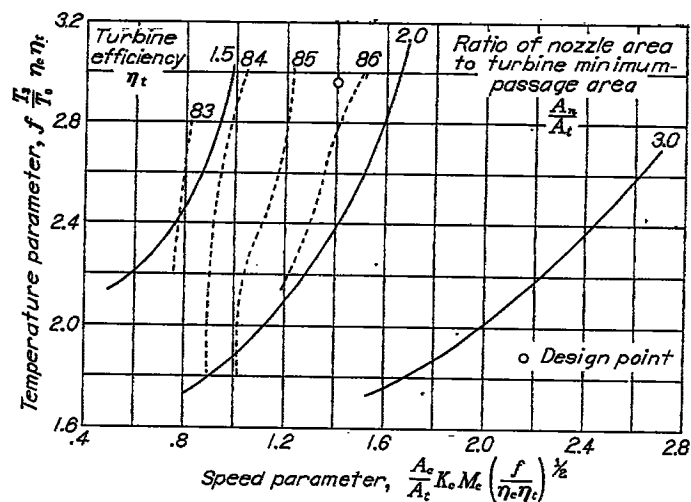

FIGURE 17.—Turbine efficiencies from experimental data superimposed on equilibrium operating lines. Ram pressure ratio, 1.00; burner pressure ratio, 1.05.

engine net thrust and component characteristics, such as compressor pressure ratio and compressor pressure coefficient.

Experimental correlation of the theory with data from several existing axial-flow-type engines was good and showed close correlation between calculated and measured performance.

Although the theoretical results are chiefly applicable to engines having a constant ratio of axial inlet-air velocity to compressor-tip velocity, these results can be used for any type of turbojet engine if the value of this ratio is known.

LEWIS FLIGHT PROPULSION LABORATORY,
NATIONAL ADVISORY COMMITTEE FOR AERONAUTICS,
CLEVELAND, OHIO, *February 25, 1949.*

APPENDIX

DERIVATION OF EQUATIONS

Diagram of turbojet engine.—The following diagram shows the location of stations in the engine:
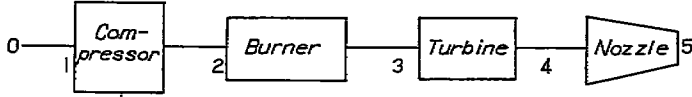
Compressor air flow.—If the ratio of compressor-inlet-air velocity to compressor-blade-tip velocity is considered constant, the equation for compressor air flow can be developed as follows:

$$\frac{Q_c}{\pi N D A_c}=K_c$$

$$Q/A_c=V_1$$

$$\pi D N=V_c$$

$$K_c=V_1/V_c$$

$$W_c=Q_1\rho_1=\rho_1 K_c V_c A_c$$

$$M_c=\frac{V_c}{\sqrt{\gamma_c R T_1}}$$

$$\rho_1=\frac{P_0}{R T_0}(r_r)^{\frac{1}{\gamma_c}}$$

$$T_1=T_0(r_r)^{\frac{\gamma_c-1}{\gamma_c}}$$

Compressor power.—The compressor power can be expressed as

$$\mathrm{hp}_c=\frac{W_c}{\eta_c}\left(\frac{\gamma_c}{\gamma_c-1}\right)\frac{R T_1}{550}\left[(r_c)^{\frac{\gamma_c-1}{\gamma_c}}-1\right]$$

$$T_1=T_0(r_r)^{\frac{\gamma_c-1}{\gamma_c}}$$

Then

$$\mathrm{hp}_c=\frac{W_c}{550\,\eta_c}\left(\frac{\gamma_c}{\gamma_c-1}\right)R T_0(r_r)^{\frac{\gamma_c-1}{\gamma_c}}\left[(r_c)^{\frac{\gamma_c-1}{\gamma_c}}-1\right] \quad (2)$$

Turbine power.—The turbine power is

$$\mathrm{hp}_t=\frac{W_t}{550}\eta_t\left(\frac{\gamma_t}{\gamma_t-1}\right)R T_3\left[1-\left(\frac{1}{r_t}\right)^{\frac{\gamma_t-1}{\gamma_t}}\right] \quad (4)$$

Therefore,

$$\frac{W_c\sqrt{T_0}}{P_0}=K_c M_c A_c(r_r)^{\frac{\gamma_c+1}{2\gamma_c}}\sqrt{\frac{\gamma_c}{R}} \quad (1)$$

Turbine air flow.—From reference 4,

$$\frac{\gamma_t-1}{2}\frac{W_t^2}{A_t^2 a_3^2 \rho_3^2}=\left[\left(\frac{C}{r_t}\right)^{\frac{2}{\gamma_t}}-\left(\frac{C}{r_t}\right)^{\frac{\gamma_t+1}{\gamma_t}}\right]$$

$$\rho_3=\frac{P_3}{R T_3}=\frac{P_0}{R T_0}\frac{P_3}{P_0}\frac{T_0}{T_3}=\frac{P_0}{R T_0}\frac{r_c r_r}{r_b}\left(\frac{T_0}{T_3}\right)$$

$$a_3=\sqrt{\gamma_t R T_3}=\sqrt{\gamma_t R T_0}\sqrt{\frac{T_3}{T_0}}$$

Then

$$\frac{W_t\sqrt{T_0}}{P_0}=\sqrt{\frac{2\gamma_t}{\gamma_t-1}}\frac{A_t}{\sqrt{R}}\left(\frac{T_0}{T_3}\right)^{\frac{1}{2}}\frac{r_c r_r}{r_b}\left[\left(\frac{C}{r_t}\right)^{\frac{2}{\gamma_t}}-\left(\frac{C}{r_t}\right)^{\frac{\gamma_t+1}{\gamma_t}}\right]^{\frac{1}{2}} \quad (3)$$

Nozzle air flow.—The nozzle-air-flow equation is determined in the same manner as equation (3):

$$\frac{W_n\sqrt{T_0}}{P_0}=\sqrt{\frac{2\gamma_t}{(\gamma_t-1)R}}\frac{A_n}{(r_t)^{\frac{\gamma_t+1}{2\gamma_t}}}\left(\frac{r_r r_c}{r_b}\right)\left(\frac{T_0}{T_3}\right)^{\frac{1}{2}}\left[\left(\frac{r_t r_b}{r_r r_c}\right)^{\frac{2}{\gamma_t}}-\left(\frac{r_t r_b}{r_c r_r}\right)^{\frac{\gamma_t+1}{\gamma_t}}\right]^{\frac{1}{2}} \quad (5)$$

Power balance.—Because $\mathrm{hp}_c=\mathrm{hp}_t$ and $W_t=f W_c$, the following expression can be developed from equations (2) and (4) for r_c:

$$(r_c)^{\frac{\gamma_c-1}{\gamma_c}}=1+f\frac{\gamma_t(\gamma_c-1)}{\gamma_c(\gamma_t-1)}\left(\frac{T_3}{T_0}\right)\frac{\eta_c\eta_t}{(r_r)^{\frac{\gamma_c-1}{\gamma_c}}}\left[1-\frac{1}{(r_t)^{\frac{\gamma_t-1}{\gamma_t}}}\right] \quad (A1)$$

Compressor-turbine air-flow balance.—Similarly, from equations (1) and (3), a second expression can be developed:

$$r_c=\frac{f K_c A_c(r_r)^{\frac{\gamma_c+1}{2\gamma_c}}r_b\sqrt{\gamma_c}M_c}{\sqrt{\frac{2\gamma_t}{\gamma_t-1}}A_t\left(\frac{T_0}{T_3}\right)^{\frac{1}{2}}r_r\left[\left(\frac{C}{r_t}\right)^{\frac{2}{\gamma_t}}-\left(\frac{C}{r_t}\right)^{\frac{\gamma_t+1}{\gamma_t}}\right]^{\frac{1}{2}}} \quad (A2)$$

Final equilibrium.—Combination of the power-balance and flow-balance equations (A1) and (A2), respectively, to eliminate r_c gives

$$\left\{1+f\frac{\gamma_t(\gamma_c-1)}{\gamma_c(\gamma_t-1)}\left(\frac{T_3}{T_0}\right)\frac{\eta_c\eta_t}{(r_r)^{\frac{\gamma_c-1}{\gamma_c}}}\left[1-\left(\frac{1}{r_t}\right)^{\frac{\gamma_t-1}{\gamma_t}}\right]\right\}^{\frac{\gamma_c}{\gamma_c-1}}\left[\left(\frac{C}{r_t}\right)^{\frac{2}{\gamma_t}}-\left(\frac{C}{r_t}\right)^{\frac{\gamma_t+1}{\gamma_t}}\right]^{\frac{1}{2}}=\frac{A_c}{A_t}f\frac{K_c M_c r_b}{(r_r)^{\frac{\gamma_c-1}{2\gamma_c}}}\left(\frac{T_3}{T_0}\right)^{\frac{1}{2}}\sqrt{\frac{\gamma_c(\gamma_t-1)}{2\gamma_t}} \quad (6)$$

Ratio of nozzle area to turbine minimum-passage area.— Combination of the nozzle and turbine mass flows yields

$$W_n = W_t$$

$$\sqrt{\frac{2\gamma_t}{(\gamma_t-1)R}}\, A_t \left(\frac{T_0}{T_3}\right)^{\frac{1}{2}}\left(\frac{r_r r_c}{r_b}\right)\left[\left(\frac{C}{r_t}\right)^{\frac{2}{\gamma_t}}-\left(\frac{C}{r_t}\right)^{\frac{\gamma_t+1}{\gamma_t}}\right]^{\frac{1}{2}}$$

$$=\sqrt{\frac{2\gamma_t}{(\gamma_t-1)R}}\,\frac{A_n}{(r_t)^{\frac{\gamma_t+1}{2\gamma_t}}}\left(\frac{r_r r_c}{r_b}\right)\left(\frac{T_0}{T_3}\right)^{\frac{1}{2}}\left[\left(\frac{r_t r_b}{r_r r_c}\right)^{\frac{2}{\gamma_t}}-\left(\frac{r_t r_b}{r_r r_c}\right)^{\frac{\gamma_t+1}{\gamma_t}}\right]^{\frac{1}{2}}$$

Then

$$\frac{A_n}{A_t}=\frac{(r_t)^{\frac{\gamma_t+1}{2\gamma_t}}\left[\left(\frac{C}{r_t}\right)^{\frac{2}{\gamma_t}}-\left(\frac{C}{r_t}\right)^{\frac{\gamma_t+1}{\gamma_t}}\right]^{\frac{1}{2}}}{\left[\left(\frac{r_t r_b}{r_r r_c}\right)^{\frac{2}{\gamma_t}}-\left(\frac{r_t r_b}{r_r r_c}\right)^{\frac{\gamma_t+1}{\gamma_t}}\right]^{\frac{1}{2}}} \qquad (7)$$

$$F=\frac{P_0 A_c}{\sqrt{T_0}}\,K_c M_c (r_r)^{\frac{\gamma_c+1}{2\gamma_c}}\sqrt{\frac{\gamma_c}{R}}\left[f\sqrt{\frac{2\gamma_t}{\gamma_t-1}\,R\,\frac{T_3}{(r_t)^{\frac{\gamma_t-1}{\gamma_t}}}\left[1-\left(\frac{r_t r_b}{r_r r_c}\right)^{\frac{\gamma_t-1}{\gamma_t}}\right]}-V_0\right]$$

$$F=P_0 K_c M_c A_c (r_r)^{\frac{\gamma_c+1}{2\gamma_c}}\sqrt{\gamma_c}\left[f\sqrt{\frac{2\gamma_t}{\gamma_t-1}\left(\frac{T_3}{T_0}\right)\frac{1}{(r_t)^{\frac{\gamma_t-1}{\gamma_t}}}\left[1-\left(\frac{r_t r_b}{r_r r_c}\right)^{\frac{\gamma_t-1}{\gamma_t}}\right]}-\frac{V_0}{\sqrt{RT_0}}\right]$$

$$\frac{F}{P_0 A_t}=\frac{A_c}{A_t}K_c M_c (r_r)^{\frac{\gamma_c+1}{2\gamma_c}}\gamma_c\left\{f\sqrt{\frac{2\gamma_t}{\gamma_c(\gamma_t-1)}\left(\frac{T_3}{T_0}\right)\left(\frac{1}{r_t}\right)^{\frac{\gamma_t-1}{\gamma_t}}\left[1-\left(\frac{r_t r_b}{r_c r_r}\right)^{\frac{\gamma_t-1}{\gamma_t}}\right]}-M_0\right\} \qquad (8)$$

Net thrust.—A convenient expression for net thrust can be developed as follows:

$$V_j=\sqrt{\frac{2\gamma_t}{\gamma_t-1}\left(\frac{P_4}{\rho_4}-\frac{p_5}{\rho_5}\right)}$$

$$V_j=\sqrt{\frac{2\gamma_t}{\gamma_t-1}\,RT_4\left[1-\left(\frac{1}{r_n}\right)^{\frac{\gamma_t-1}{\gamma_t}}\right]}$$

$$r_n=\frac{P_4}{P_5}=\frac{P_4}{P_3}\frac{P_3}{P_2}\frac{P_2}{P_1}\frac{P_1}{P_5}$$

$$=\frac{1}{r_t}\frac{1}{r_b}r_c r_r$$

$$V_j=\sqrt{\frac{2\gamma_t}{\gamma_t-1}\,RT_4\left[1-\left(\frac{r_t r_b}{r_c r_r}\right)^{\frac{\gamma_t-1}{\gamma_t}}\right]}$$

$$T_4=\frac{T_3}{(r_t)^{\frac{\gamma_t-1}{\gamma_t}}}$$

$$F=f W_c V_j - W_c V_0$$

REFERENCES

1. Goldstein, Arthur W.: Analysis of Performance of Jet Engine from Characteristics of Components. I-Aerodynamic and Matching Characteristics of Turbine Component Determined with Cold Air. NACA Rep. 878, 1947. (Formerly NACA TN 1459.)
2. Kochendorfer, Fred D., and Nettles, J. Cary: An Analytical Method of Estimating Turbine Performance. NACA Rep. 930, 1949. (Formerly NACA RM E8I16.)
3. Palmer, Carl B.: Performance of Compressor-Turbine Jet-Propulsion Systems. NACA ACR L5E17, 1945.
4. Taylor, G. I., and Maccoll, J. W.: Aerodynamic Theory, W. F. Durand, ed., vol. III, div. II, p. 224. Reprinted, C. I. T., 1943.